

Research Article

Yao Zhou, Jufan Zhang and Fengzhou Fang*

Stray light analysis and design optimization of geometrical waveguide

<https://doi.org/10.1515/aot-2020-0059>

Received October 19, 2020; accepted December 17, 2020;
published online January 5, 2021

Abstract: Waveguide technology has great prospects of development in optical see-through near-eye displays with larger field of view, lower thickness and lighter weight than other conventional optical technologies. However, the stray light is usually inevitable in current optical design and manufacturing, causing a poor imaging quality. In this paper, the principle and structures of stray light generation are analyzed, and the causes are discussed by non-sequential ray-tracing with mass precision calculation. From the ray-tracing, the suppression of stray light by optimizing design and manufacturing are achieved. A 2 mm-thickness geometrical waveguide with partially reflective mirror array is designed. The field of view of the optimized geometrical waveguide reaches 47° with 10 mm at exit pupil diameter and 20 mm at eye relief.

Keywords: geometrical waveguide; optical design; stray lights; vision optical system.

1 Introduction

Driven by technology development, the optical see-through near-eye displays have attracted more attention in recent decades. Optical see-through near-eye displays potentially span various areas such as medical devices, education, aviation and entertainment. The typical

applications include Head-mounted Display (HMD) and Augmented Reality (AR), etc. Commercial products are available from corporations like Microsoft HoloLens [1], Lumus [2], Sony [3], Waveoptics [4] and LingxiAR [5]. For the optical see-through display shown in Figure 1, the visual information is projected by a projector and displayed in front of the eye by a transparent optical element without blocking the view to the real world. To achieve the sense of immersion, various optical elements have been applied such as prism, freeform optics, birdbath, diffractive optics and optical waveguide [6–8]. Compared with to conventional optical technology, optical waveguide can meet superior optical performance, larger the field of view (FOV) with compact optical elements, along with high-resolution, large eye relief (ERF), small thickness and light-weight. Waveguide technology is classified into geometrical waveguide and diffractive waveguide by different coupler.

The earlier patent applying the refractive and reflective extraction was described by Thomson-CSF in 1991 [9]. In recent years, Microsoft Hololens and Magic leap One have driven the development of holographic waveguide and diffractive waveguide commercially. Lumus, Digilens and Lingxi have also released geometrical waveguide products [9–11].

In this paper, the principle and structures of optical see-through display are analyzed, and the causes and suppression methods are discussed. A geometrical waveguide is designed and optimized.

2 Waveguide system

For the geometrical waveguide system, as shown in Figure 2a, the visual information is projected by a light source, then collimated and coupled into waveguide. The light can be totally reflected internally within two edges of waveguide component and coupled out to observer's eyes till it transfer to partially reflective mirror array (PRMA), which break the total internal reflections (TIRs). The geometrical waveguide works as an entrance pupil expander, which is a separate element independent of the imaging system as shown in Figure 2b. This property of the

*Corresponding author: Fengzhou Fang, Centre of Micro/Nano Manufacturing Technology (MNMT-Dublin), School of Mechanical & Materials Engineering, University College Dublin, Dublin 4, Dublin, Ireland; and State Key Laboratory of Precision Measuring Technology and Instruments, Centre of Micro/Nano Manufacturing Technology (MNMT), Tianjin University, Tianjin 300072, China, E-mail: fengzhou.fang@ucd.ie. <https://orcid.org/0000-0002-8716-5988>

Yao Zhou and Jufan Zhang, Centre of Micro/Nano Manufacturing Technology (MNMT-Dublin), School of Mechanical & Materials Engineering, University College Dublin, Dublin 4, Dublin, Ireland

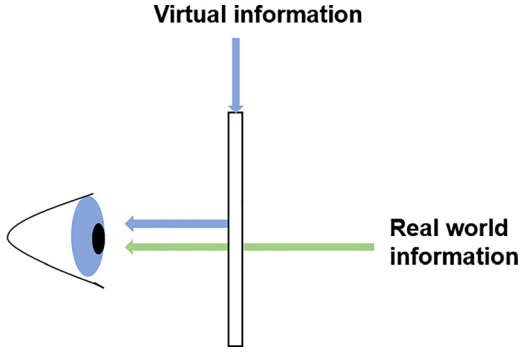


Figure 1: Optical see-through display.

waveguide has great advantages in optimizing the design and appearance of the headset. However, several exit pupils increase the total area of exit pupil, which decrease the luminous flux at each exit pupil. The optical efficiency of the waveguide is low, and a powerful projector is required.

Figure 2a shows the schematic diagram of the geometrical waveguide near-eye display, where n is the index of the base material, D is the thickness of the waveguide, θ is the angle between the edge of waveguide and in-coupler. The angle between the out-coupler and the edge of the waveguide is θ . There are five mirrors (out-couplers) in the waveguide. The maximum field angle along the direction of entrance pupil expander (EPD) can be defined as Eq. (1). EPD is the best observation area on the exit pupil plane.

$$\tan \Omega_{max} = \frac{N \cdot D}{\tan \theta} - EPD, \tag{1}$$

where the N is the number of PRMA. The FOV of the waveguide is Eq. (2).

$$FOV = 2 \tan^{-1} \frac{N \cdot D}{2ERF} - EPD \tag{2}$$

The lights transfer inside by TIR, which means the lights' inside angle with the edge ω_2 (shown in Figure 3) must be bigger than the critical angle θ_c , which must satisfy the following formula:

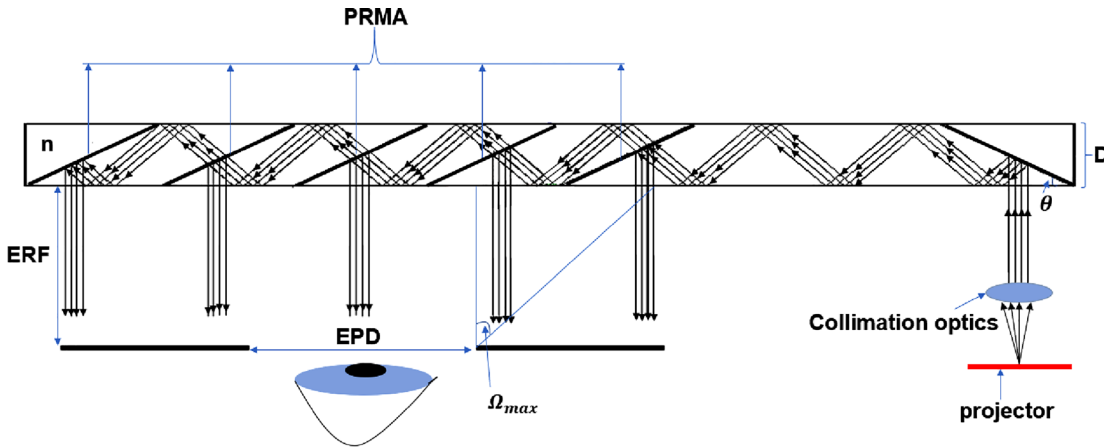
$$\theta_c = \sin^{-1} \left(\frac{1}{n} \right), \tag{3}$$

$$\omega_2 = 2\theta - \omega_1 > \theta_c, \tag{4}$$

where ω_1 is the refractive angle of the light along the entrance pupil expansion in the waveguide. Any angle lower than the critical angle cannot be reflected within the waveguide. In engineering optics, the refractive index of air is often regarded as 1. Thus, it is derived as the following

$$\theta > \frac{\sin^{-1} \left(\frac{1}{n} \right) + \omega_1}{2}. \tag{5}$$

From above, it is obtained that the bigger refractive index of the substrate results in larger FOV when keeping the other variables constant. The whole length of the one



a. Schematic diagram of the geometrical waveguide near-eye display



b. The process of the system

Figure 2: The geometrical waveguide system.

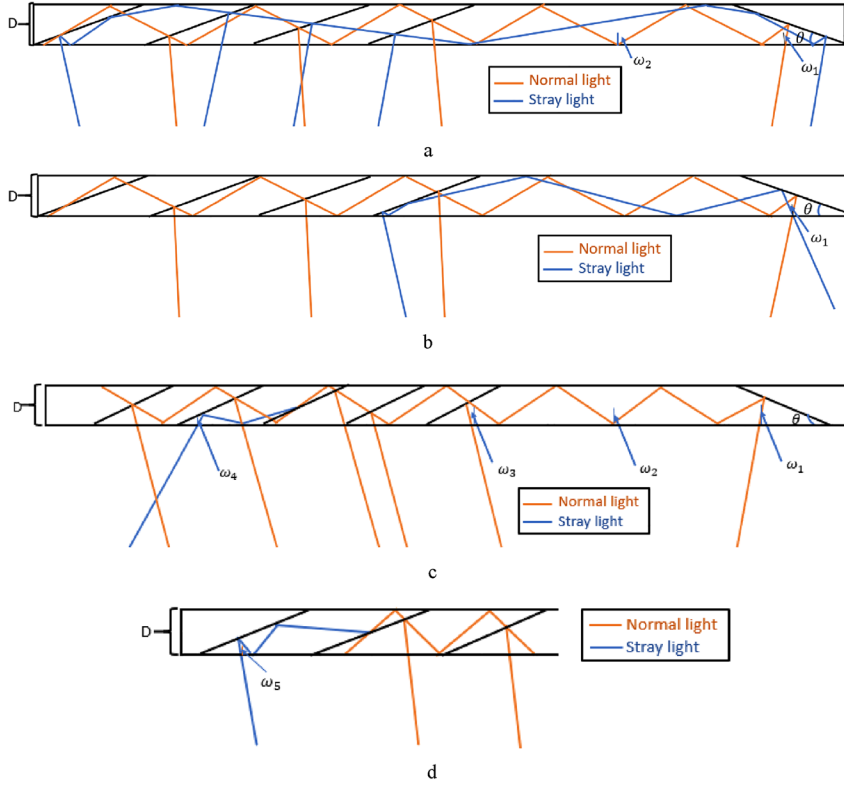


Figure 3: Stray lights in geometrical waveguide (a) twice reflection at in-coupler; (b) twice reflection at out-coupler; (c) and (d) lights are reflected by the back of out-coupler.

side waveguide cannot be too long, as expressing in Eq. (6). Usually, the maximum number is set as L_{whole} , which is set for the waveguide before reaching the out-couplers.

$$L_{whole} = \frac{N*D}{\tan \theta} + \frac{m*D}{\tan(2\theta - \omega_1)} < 60mm, \quad (6)$$

where m is the number of refractions of the light before reaching the first out-coupler. Hence, it is derived below:

$$m < \left(\frac{60mm}{D} - \frac{N}{\tan \theta} \right) * \tan(2\theta - \omega_1). \quad (7)$$

To increase the range of eye moving, the exit pupil diameter (EPD) is usually 10 mm. ERF is set to 20 mm to satisfy the observers with glasses. People pursue large FOV, according to Eq. (2), the bigger D , smaller θ , smaller EPD and ERF could reach the larger FOV. However, in practical application, larger FOV, thinner waveguide and bigger EPD and ERF are all expected. Thus, the parameters selection is a trade-off process depending on different application focus.

3 Stray light analysis

The waveguide works in expanding the light information from projector. The pupil plane is like the exit pupil plane of the image. The pupil could intercept the complete

image information from this plane, which could be transmitted to retina by lens. Therefore, the light from the same angle will cover one visual cell, like a pixel in the imager sensor, without any double shadows or ghost images [12].

According to the geometry of the waveguide, the pupil is expanded by PRMA. In this process, some unwanted ghost images would occur due to the inconsistency of the angle of the waveguide within-surface array, so the stray light would be generated by these inevitable reflections. The contrast, modulation transfer function (MTF) and sharpness of the image would be greatly reduced by stray lights and energy distribution of the image plane would undergo a significant change. Severely, the target image would be annihilated in the background stray light. The stray light would become stronger when FOV increases in the direction of entrance expansion. The ghost image in the edge is more obvious than it in the centre. There are several cases of the stray lights. The first case is caused by twice reflection at the in-coupler, as shown in Figure 3a. All lights just need to be reflected once by in-coupler and the second reflection change the original direction of the normal lights and cause stray lights. The first case usually happens when

$$\omega_1 < \pi/2 - 3\theta. \quad (8)$$

The second case is caused by twice reflection by one out-coupler, as shown in Figure 3b. All lights

should be coupled out to observer's eye by once reflection at out-coupler. But some lights may not break the TIR condition after the first reflection at the out-coupler and hit the same out-coupler again. In this situation, the lights may not transfer in the original direction and become stray lights. The second case happens when

$$\omega_1 < 3\theta - \pi/2. \quad (9)$$

As shown in Figure 3a, the first case may also cause the second case at the edge of the waveguide. The third case and the fourth case are both caused by reflection at the back of the out-coupler, as shown in Figure 3c and Figure 3d, respectively. For ideal design, all lights, no matter from projector or from real world, should pass through the back of out-couplers. But the lights reflected on the back of the out-coupler still transfer within the waveguide and then may be coupled out to observer after once or twice reflected by the next out-coupler (once reflection by next out-coupler in Figure 3c, twice reflection in Figure 3d).

From Figure 3c and Eq. (4), the angle of normal light along the expansion direction before it passes through the waveguide ω_3 can be derived as

$$\omega_3 = \omega_1. \quad (10)$$

The angle of third and fourth cases of stray light along the expansion direction before it passes through the waveguide ω_4 and ω_5 can be derived as

$$\omega_4 = \pi - 6\theta + \omega_1, \quad (11)$$

$$\omega_5 = 6\theta - 3\pi/2 + \omega_1, \quad (12)$$

which happens when

$$\omega_1 < 4\theta - \pi/2 \text{ (thirdcase)}, \quad (13)$$

$$\omega_1 > 4\theta - \pi/2 \text{ (fourthcase)}. \quad (14)$$

From above, the stray lights can be concluded by Figure 4. When θ and ω_1 are set up, the kinds of stray lights would be determined. Then the stray lights can be solved in a targeted manner. Green line is first case stray light, blue line is second case stray light area, red line is third stray light area and the black line is the fourth case of stray light.

4 Suppression by optical design

To suppress the first case of stray light, part of the in-coupler Y could be removed, or the edge of the waveguide X

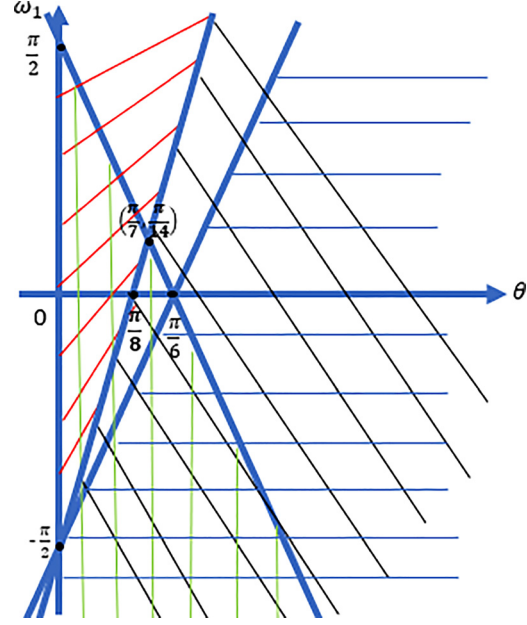


Figure 4: All kinds of stray lights (green line is 1st stray light, blue line is 2nd stray light, red line is 3rd stray light and black line is 4th stray light).

could be blocked, which shows the critical condition as seen in Figure 5. The light hits the edge of the in-coupler after its' reflected by in-coupler. X and Y part can be expressed as:

$$Y = \frac{D}{\sin \theta} - \frac{2D \sin(2\theta - \omega_1)}{\cos(\omega_1 - \theta)}, \quad (15)$$

$$X = \frac{Y \cos(\omega_1 + \theta)}{\cos \omega_1}. \quad (16)$$

For the second case of stray light, the abnormal light would be suppressed when first stray light was eliminated and the angle meets Eq. (9).

The suppression method of third and fourth condition are mainly in the coating on the out-coupler. Stray light is caused by the convergence of real light rays, which is reflected from the optical working surface on the image surface, usually normal light passing through even

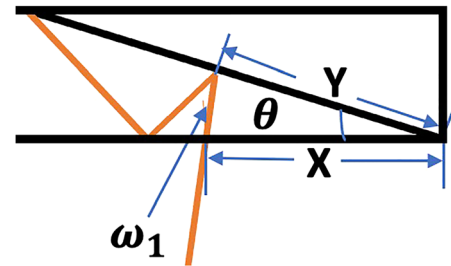


Figure 5: Suppression of first stray light.

times on the working surface. For imaging optical systems, stray light increases the noise on the image surface and decreases the contrast of the image. The coating film can weaken the reflection of the beam with large incident angle as much as possible and divide the beam with small incident angle in a certain proportion, so as to expand the field of view.

As shown in Figure 6, the light from one side can be reflected by the film while part of which could be transmitted through the film, where the reflection and transmission ratio is different on every film). And the light from the other side can totally transmits through the film. The selection of coating materials should consider such issues as the low absorption rate in the required band, the matching degree between the film layer and the incident medium, and the refractive index of the base. Usually, the material with high refractive index is H_4 and from the angle of refractive index matching, MgF_2 is selected as the material with low refractive index [13].

Besides, if the stray lights in third and fourth condition can be transmitted out of EPD, they can be ignored, as shown in Eq. (17) and Eq. (18).

$$L_{Stray} = ERF * \tan[\sin^{-1}(n_1 * \sin \omega_4)] \geq EPD, \quad (17)$$

$$L_{Stray} = ERF * \tan[\sin^{-1}(n_1 * \sin \omega_5)] \geq EPD. \quad (18)$$

from which, the ω_4 and ω_5 could be derived to suppress these two conditions.

5 Suppression by manufacturing

Besides the stray lights in the waveguide system, there are some situations of stray lights caused by manufacturing. The errors in manufacturing break the original light path

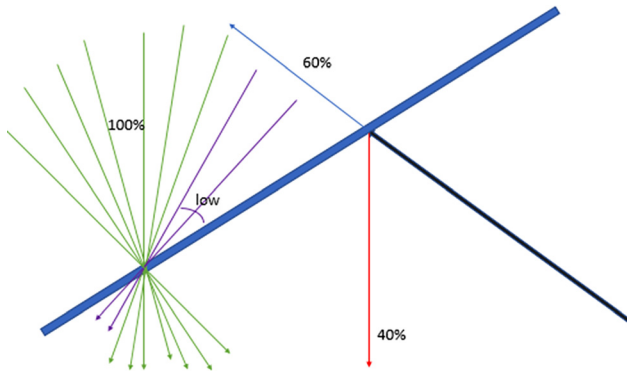


Figure 6: Selection of the coating film on out-coupler (red line is reflected light, blue line is transmitted light, green line is totally transmitted light and purple line is transmitted light with very low percentage).

and cause stray light. As shown in Figure 7, the manufactured waveguide has a parallelism error between two edges, which is noted by angle Δ . After the light hits the waveguide edge with error, it continues to transmit in the wrong way. And everytime the light hits the error edge, the transmission deviates more from the normal angle [14].

Eq. (19) expresses the angle error before the light through-out the waveguide along the normal direction.

$$\Delta\omega_3 = 2\Delta$$

$$\Delta\omega_4 = 3\Delta$$

$$\Delta\omega_5 = 4\Delta$$

... ..

$$\Delta\omega_{q-1} = q * \Delta. \quad (19)$$

where the q is the number of hits of light at the error edge of waveguide.

As the angular resolution of the human eye is $60''$ [15], the manufacturing error could be accepted if largest angle error is below $60''$, any angle beyond which causes ghost image,

$$\sin^{-1}[n * \sin(q * \Delta)] < 60'', \quad (20)$$

$$\Delta < \frac{\sin^{-1}\left[\frac{\sin 60''}{n}\right]}{q}. \quad (21)$$

The length of waveguide and the number of the out-coupler determine q . Thus, only when the manufacturing error meets Eq. (21), observers could get the virtual information with no ghost image in this type.

The same light is coupled out by PRMA in parallel. The parallelism of the out-couplers is crucial. If there is a parallelism error of out-couplers, the light transmits deviates from the normal angle, as shown in Figure 8. There are two kinds of parallelism errors, upper and lower than the right angle.

Eq. (22) express the parallelism error in upper and lower angle than the normal angle.

$$\Delta\omega_5 = 2\Delta',$$

$$\Delta\omega_6 = 2\Delta''. \quad (22)$$

where Δ' is lower angle than the normal angle and Δ'' is the upper angle than the normal angle.

$$\sin^{-1}[n * \sin(\Delta\omega_5 \text{ or } \Delta\omega_6)] < 60'', \quad (23)$$

$$\Delta' / \Delta'' < \frac{\sin^{-1}\left[\frac{\sin 60''}{n}\right]}{2}. \quad (24)$$

When the manufacturing error meets Eq. (23), the virtual

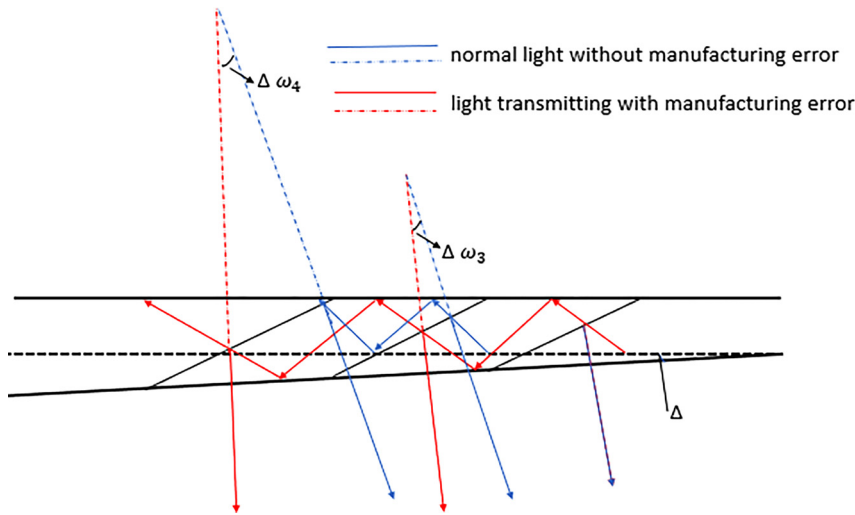


Figure 7: Stray light caused by manufacturing error at substrate of waveguide.

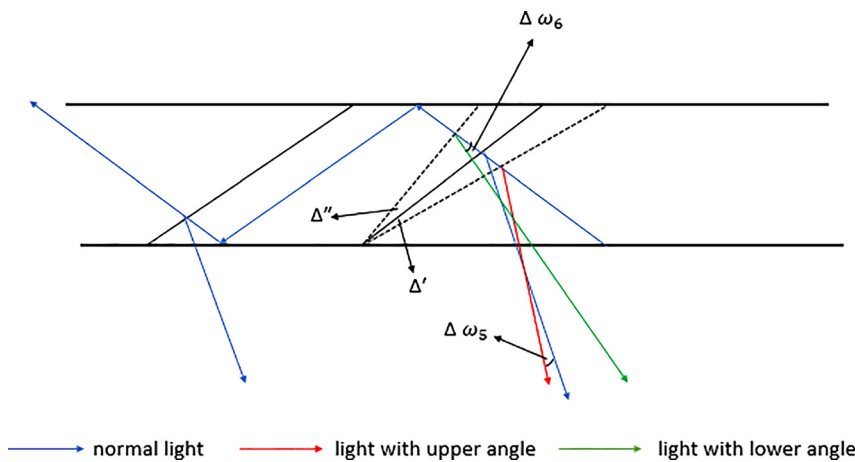


Figure 8: Stray light from the manufacturing at out-coupler of waveguide.

information could be seen completely by human eyes with no ghost image in this type.

6 Design and simulation

The parameters selection is a trade-off process depending on the application. According to above analysis, to provide a thinner thickness and larger FOV of a wearable geometrical waveguide, the parameters in the design are listed in Table 1. Based on the above parameters, the FOV can be calculated as 47° from Eq. (26).

Table 1: parameters of the geometrical waveguide.

n	ω_1	θ	N	D (mm)	EPD (mm)	ERF (mm)
>1.66	0°	20	8	2	10	20

In order to eliminate the overlapping image, every light is coupled out once by every out-coupler, thus, only the active part of the partially reflective surface is embedded in the substrate, as shown in Figure 9. The reflective surfaces are adjacent to each other and eyes will extract the full image from the exit pupil plane. Thus, there will be no holes of the projected image by the non-overlap surfaces. The out-coupler design affects the FOV. The active part of out-coupler can be expressed as

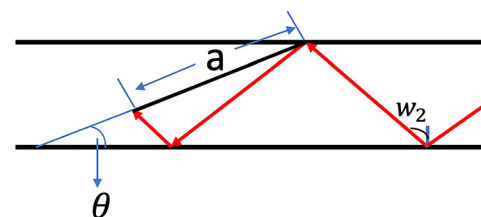
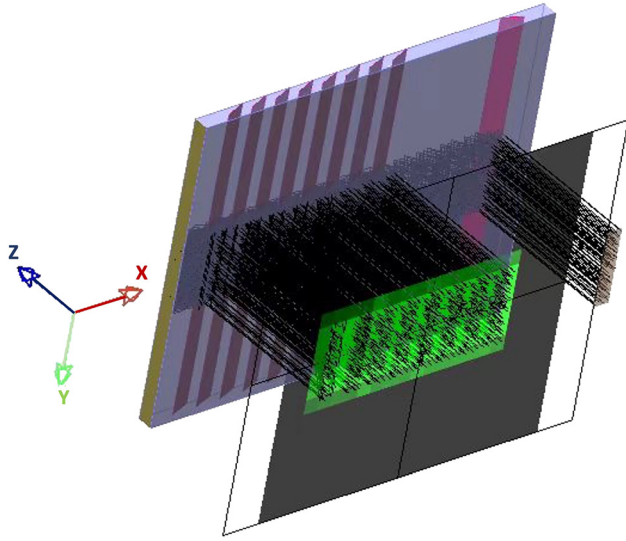


Figure 9: Active part of out-coupler.

Table 2: The ratio of transmittance and reflectance.

Out-coupler	1st	2nd	3rd	4th	5th	6th	7th	8th
Reflectance	12.5%	14.3%	16.7%	20%	25%	33%	50%	100%
Transmittance	87.5%	85.7%	83.3%	80%	75%	67%	50%	0

**Figure 10:** Schematic diagram of the optimized geometrical waveguide.

$$a = \frac{2D \sin(2\theta - \omega_1)}{\cos(\omega_1 - \theta)} \quad (25)$$

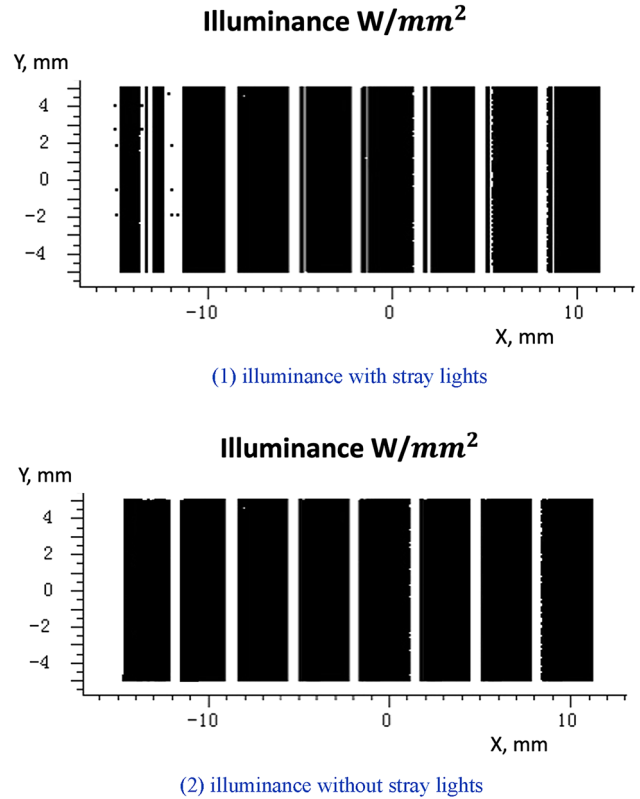
and the FOV of new designed system can be derived as

$$FOV_{design} = 2 \tan^{-1} \frac{N * 2D \tan(2\theta - \omega_1) - EPD}{2ERF} \quad (26)$$

The ratio of transmittance and reflectance of the film on every out-coupler should follow Table 2 to make sure the uniform of the illuminance.

Based on above, the schematic diagram of the optimized geometrical waveguide is shown in Figure 10. The wavelength of the light source is 550 nm with 2.3×10 mm area. The luminous flux is 679.55 Lumen with uniform angle distribution and volume distribution. The weight coefficient is 1. For the ray tracing, the maximum number of hits at per surface is 1000.

Figure 11(1) shows the illuminance of the waveguide with no optimization for the coating at the exit pupil of the system. The light is quite uneven distribution, the field loss occurs at the edge of the out-couplers, which cause lots of ghost images. Figure 11(2) shows the illuminance of the optimized geometrical waveguide with the same light source at exit pupil, as designed in Table 2. From the ray-tracing analysis, the light distribution is uniform and the

**Figure 11:** Scatterer distribution diagram of illuminance, (1) is the illuminance with stray lights and (2) is light illuminance without stray lights, the unit is W/mm^2 .

stray light is greatly suppressed. The projected light is expanded several times by folding and unfolding process. The gap between every surface is below the resolution of human eyes. Figure 12 shows the angular distribution of the optimized system, which effectively suppress the stray lights and expands the field-of-view for the system.

However, the manufacturing process is rather complicated, including coating, stacking, slicing, lapping and polishing, shaping and testing. For example, for the coating process of the half-reflection-half-transmission mirror array, every ratio of the R/T is different from ensure the uniform light output. For the manufacturing, all light transfers by polarization from the projector, thus, the number of the coating layers may be dozen or even dozens on per mirror, after which, the stacking and shaping are very important, because the parallelism between the

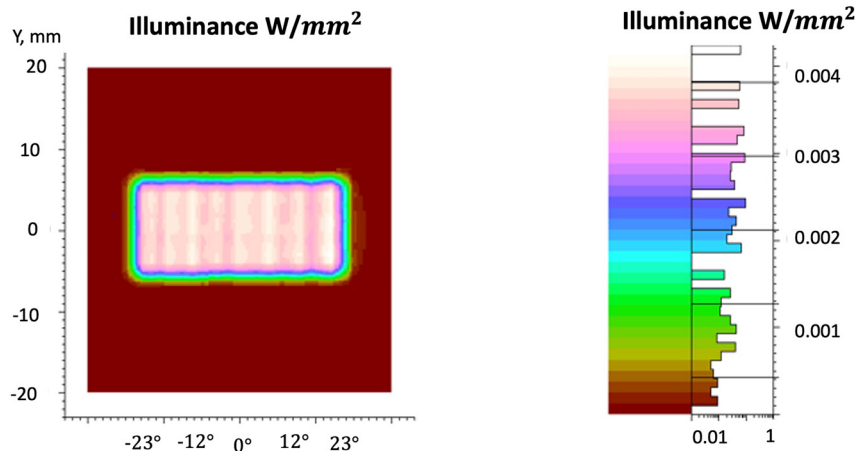


Figure 12: The angular distribution of the optimized system, the unit is W/mm^2 .

couplers and the angle of the cutting affect the quality of the images. Therefore, even if each step of the process can achieve high yield, the combined total yield of these dozens of steps is still a challenge. Failure of each process may lead to defects in the imaging, such as background black stripe, uneven brightness, ghost image, etc.

7 Conclusion

The relationship between all parameters within a geometrical waveguide are studied. The causes of stray lights are analyzed and divided by incident angle and angle between substrate and in-coupler. The suppression methods are developed based on different types of stray lights. A geometrical waveguide is designed and optimized to minimize stray light and achieve large FOV. The FOV of the optimized geometrical waveguide achieved is 47° with 10 mm at exit pupil diameter (EPD), 20 mm at ERF and 2 mm in thickness. The manufacturing tolerance is also discussed to obtain more precise light path. The design and analysis of two-dimensional geometrical waveguide is ongoing to further improve the optical see-through near-eye display.

Acknowledgments: The authors would like to thank the financial support from the Science Foundation Ireland (SFI) (No. 15/RP/B3208) and the “111” Project by the State Administration of Foreign Experts Affairs and the Ministry of Education of China (No. B07014).

Author contributions: All the authors have accepted responsibility for the entire content of this submitted manuscript and approved submission.

Research funding: None declared.

Conflict of interest statement: The authors declare no conflicts of interest regarding this article.

References

- [1] *Microsoft HoloLens*, 2020. Available at: <https://www.microsoft.com/en-us/hololens>.
- [2] *Lumus*, 2020. Available at: <https://lumusvision.com/>.
- [3] *Sony*, 2020. Available at: <https://www.sony.net/united/apptech/>.
- [4] *Waveoptics*, 2020. Available at: <https://enhancedworld.com/>.
- [5] *Lingxi AR*, 2020. Available at: <http://www.lx-ar.com/en/>.
- [6] Q. Hou, Q. Wang, D. Cheng, and Y. Wang, “Geometrical waveguide in see-through head-mounted display: a review,” *Proc. SPIE*, vol. 21, p. 100210C, 2016.
- [7] J. P. Rolland, and H. Hua, “Head-mounted display systems,” *Encycl. Opt. Eng.*, vol. 2, pp. 1–13, 2005.
- [8] B. Kress, and T. Starner, “A review of head-mounted displays (HMD) technologies and applications for consumer electronics,” in *Photonic Applications for Aerospace, Commercial, and Harsh Environments IV*, vol. 8720, International Society for Optics and Photonics, 2013, p. 87200A.
- [9] *DigiLens*, 2020. Available at: <https://www.digilens.com/press-release/digilens-unveils-augmented-reality-smartglasses/>.
- [10] *Magic Leap 1*, 2020. Available at: <https://www.magicleap.com/en-us/magic-leap-1>.
- [11] Y. Zhang, and F. Z. Fang, *Development of Planar Diffractive Waveguides in Optical See-Through Head-Mounted Displays*, The Netherlands: Precision Engineering, 2019.
- [12] Y. Zhou, J. Zhang, and F. Z. Fang, “Advances in the design of optical see-through displays,” *Adv. Opt. Technol.*, vol. 1, 2020.
- [13] F. Z. Fang, Y. Cheng, and X. Zhang, “Design of freeform optics,” *Adv. Opt. Technol.*, vol. 2, pp. 445–453, 2013.
- [14] F. Z. Fang, X. Zhang, A. Weckenmann, G. Zhang, and C. Evans, “Manufacturing and measurement of freeform optics,” *CIRP Ann.*, vol. 62, pp. 823–846, 2013.
- [15] M. Born, and E. Wolf, *Principles of Optics: Electromagnetic Theory of Propagation, Interference and Diffraction of Light*, The Netherlands: Elsevier, 2013.

Bionotes

Yao Zhou

Centre of Micro/Nano Manufacturing Technology (MNMT-Dublin),
School of Mechanical & Materials Engineering, University College
Dublin, Dublin 4, Dublin, Ireland

Yao Zhou is currently pursuing the Ph.D. degree at University College Dublin. Her research interests include optical design and manufacturing of geometrical waveguide and relevant advanced optical see-through display system.

Jufan Zhang

Centre of Micro/Nano Manufacturing Technology (MNMT-Dublin),
School of Mechanical & Materials Engineering, University College
Dublin, Dublin 4, Dublin, Ireland

Jufan Zhang is the research fellow of University College Dublin. He mainly focuses on the research of micro/nano manufacturing, design and fabrication of advanced optical systems, micro/nano functional

surface textures. He is applying the research outcomes of advanced optical solutions on various biomedical and optical applications and was awarded several major funding.

Fengzhou Fang

Centre of Micro/Nano Manufacturing Technology (MNMT-Dublin),
School of Mechanical & Materials Engineering, University College
Dublin, Dublin 4, Dublin, Ireland

State Key Laboratory of Precision Measuring Technology and
Instruments, Centre of Micro/Nano Manufacturing Technology
(MNMT), Tianjin University, Tianjin 300072, China

fengzhou.fang@ucd.ie

<https://orcid.org/0000-0002-8716-5988>

Fengzhou Fang is a joint professor of Centre of Micro/Nano Manufacturing Technology (MNMT) at Tianjin University and University College Dublin. He has conducted both fundamental studies and application development in the areas of micro/nano machining, optical freeform design and manufacturing, and ultra-precision machining and measurement benefiting a variety of industries in medical devices, bio-implants, optics and mold sectors.